VIP

Is It Possible To Get High T_C Magnets with Prussian Blue Analogues? A Theoretical Prospect

Eliseo Ruiz,*[a] Antonio Rodríguez-Fortea,[a] Santiago Alvarez,[a] and Michel Verdaguer[a, b]

Abstract: Theoretical methods based on density functional theory have been employed to search for Prussian blue analogues with Curie temperatures higher than the ones reached today. Our study suggests several possible cyano-bridged compounds as candidates to present stronger exchange coupling and higher ordering temperatures than the well known $Cr^{III}V^{II}$ derivatives.

Keywords: density functional calculations · electronic structure · magnetic properties · molecular magnets · Prussian blue analogues

The search for molecule-based compounds with long-range magnetic order at room temperature is one of the current goals of research in the field of molecular magnetism.[1,2] Presently, two families of molecule-based materials behave as room-temperature magnets. The first family can be formulated as $V[TCNE]_x \cdot y\,CH_2Cl_2$ and was obtained by Manriquez et al. when looking for vanadium-based charge-transfer materials. The samples decompose below T_C and a complete characterization of this system is still in progress.[3] The second family of materials that behave as room-temperature magnets, $V[Cr(CN)_6]_x \cdot n\,H_2O$, was obtained in 1995 by Ferlay et al.[4] This amorphous Prussian blue analogue has a Curie temperature of 315 K and a low magnetization at saturation (0.15 μ_B). It is an air-sensitive compound that contains V^{II} and V^{III} cations. Other members of the Prussian blue family with vanadium and chromium cations have since been obtained by other authors,[5] and these have higher Curie temperatures[5,6] and saturation magnetizations in line with their stoichiometry.[7,8] Two significant improvements of the synthetic procedure have led to better organized samples. Thus, a sol–gel approach and the use of potassium countercations allowed Girolami and Holmes to get a crystalline analogue with which a T_C value of 376 K was reached, the highest in the series.[6] On the other hand, the use of catalytic amounts of V^{III} during the synthesis allowed Garde et al. to obtain stoichiometric $Cr^{III}V^{II}$ compounds presenting the expected magnetization at saturation.[7]

Few theoretical studies have been devoted to the electronic structure and magnetic behavior of the Prussian blue analogues that show magnetic order at room temperature, probably because its exact crystal structure is unknown and because the symmetry of the real compounds is low. The first theoretical studies[9,10] were reported by the same authors who prepared the compound, by using the extended-Hückel method for dinuclear models. They applied the Kahn–Briat model[11,12] and attributed the exchange interaction to the overlap between magnetic orbitals through the π system. Siberchicot et al. employed the augmented spherical waves (ASW) method to perform calculations and analyzed the spin distribution in periodic structures of two well-characterized Prussian blue analogues of formula $CsM[Cr(CN)_6]$ (M = Mn, Ni).[13] Hartree–Fock calculations for idealized periodic models of $KM[Cr(CN)_6]$ ($M = V^{II}$, Mn^{II} and Ni^{II}) and $Cr[Cr(CN)_6]$ were reported by Harrison et al. during studies of the exchange coupling and the electronic structure of these materials.[14] Nishino et al. employed density functional methods for a molecular model $[(NC)_6\text{-M-CN-M}'\text{-}(CN)_6]$ to study the exchange interactions, and their results compare well with experimental data of six different Prussian blue analogues ($M = Cr^{III}$, $M' = V^{III}$, Cr^{III}, V^{II}, Mn^{II}, Ni^{II}, and $M = V^{II}$, $M' = Mn^{II}$).[15,16] Weihe and Güdel have performed a study of the exchange coupling in Prussian blue analogues using a valence bond configuration interaction (VBCI)

[a] Dr. E. Ruiz, Dr. A. Rodríguez-Fortea, Prof. Dr. S. Alvarez, Prof. Dr. M. Verdaguer
Departament de Química Inorgànica and
Centre Especial de Recerca en Química Teòrica (CeRQT)
Universitat de Barcelona
Martí i Franquès 1–11, 08028 Barcelona (Spain)
Fax: (+34) 934-907-725
E-mail: eliseo.ruiz@qi.ub.es

[b] Prof. Dr. M. Verdaguer
Laboratoire CIM2, CNRS Unit 7071, Case 42
Université Pierre et Marie Curie
4 Place Jussieu, 75252 Paris (France)

 DOI: 10.1002/chem.200400821

model and some parameterization to obtain estimates of the critical temperatures for such compounds.[17]

According to well-understood orbital rules,[10,18] exchange interactions between two transition-metal atoms with localized electrons mediated by bridging ligands are antiferromagnetic (i.e., electrons in the two metal atoms prefer to align their spins in an antiparallel way) if they involve electrons in d orbitals of the same symmetry (e.g., t_{2g} orbitals in octahedrally coordinated metals), but ferromagnetic (i.e., parallel spins) between orbitals of different symmetry (e.g., t_{2g} in one metal and e_g in the other). Notice that the symmetry notations used here are the ones for an idealized local O_h point group on each metallic center, suitable for a three-dimensional material, but do not represent a precise symmetry label in a dinuclear complex or a two-dimensional compound. Although exceptions to these simple rules exist and have been analyzed by Tsukerblat in the framework of the Anderson model,[19–21] most of the presently available Curie temperatures for Prussian blue analogues (Table 1) agree with those expectations. Thus, among the compounds with high ordering temperatures one finds C-coordinated Cr^{III} and N-coordinated V^{II}, both metal ions having a t_{2g}^3 electron configuration, a situation for which the strongest antiferromagnetic interaction and the highest T_C are to be expected.[9,10,17] Antiferromagnetic coupling in cubic Prussian blue analogues $AM'[M(CN)_6]$ (Figure 1, left), where A is an alkaline metal cation and both M and M′ are d^3 ions, should result in cancellation of the two local spins ($S + S' = 3/2 - 3/2 = 0$) below the magnetic ordering temperature and one would be left with a diamagnetic behavior. However, in the experimentally characterized $A_zM'[M(CN)_6]_x$ compounds, the stoichiometric ratio between the two metals is $1:x$ and a net spin of $|3(1-x)|/2$ results, responsible for a net magnetization below T_C. It follows that, for t_{2g}^3 ions, the closer the M′:M stoichiometry is to 1:1, the smaller the net magnetization is, as actually found by Holmes and Girolami.[6]

With all the other paramagnetic pairs implied in ferrimagnetically ordered systems, the Curie temperatures are lower than with Cr^{III}–V^{II}. An alternative way to obtain a net magnetization in a Prussian blue with $AM'[M(CN)_6]$ stoichiometry consists of having ferromagnetic coupling between M and M′. According to the orbital rules discussed above, the electron configurations corresponding to the most efficient ferromagnetic interaction (and highest ferromagnetic ordering) are $M(t_{2g}^3)$ and $M'(t_{2g}^6 e_g^2)$. Experiment reveals (Table 1) that this is a much less effective strategy, since the ordering temperatures achieved in this way are below 90 K (Table 1). To find Prussian blue analogues with the highest possible ordering temperature, it seems appropriate to search for the strongest antiferromagnetic coupling constant J between

Abstract in Spanish: *Métodos teóricos basados en la Teoría del Funcional de la Densidad se han empleado en la búsqueda de compuestos de la familia de los Azules de Prusia con temperaturas de Curie más altas que en los sistemas conocidos actualmente. Nuestro estudio sugiere que varios compuestos con puentes cianuro no sintetizados todavía son buenos candidatos a presentar un acoplamiento de intercambio más fuerte y una temperatura de ordenamiento magnético más alta que los compuestos de $Cr^{III}V^{II}$ ampliamente estudiados.*

Table 1. Experimental T_C [K] values for some Prussian blue analogues.

MM′	Compound	Configuration	T_c	Ref.
$Cr^{III}V^{II}$[a]	$KV[Cr(CN)_6]\cdot 2H_2O$	t_{2g}^3–t_{2g}^3/t_{2g}^2	376	[6]
$Cr^{III}V^{II}$/V^{III}	$K_{0.058}V[Cr(CN)_6]_{0.79}(SO_4)_{0.058}$	t_{2g}^3–t_{2g}^3/t_{2g}^2	372	[5]
	$K_{0.50}V[Cr(CN)_6]_{0.95}\cdot 1.7H_2O$	t_{2g}^3–t_{2g}^3/t_{2g}^2	350	[5]
	$V[Cr(CN)_6]_{0.86}\cdot 2.8H_2O$	t_{2g}^3–t_{2g}^3/t_{2g}^2	315	[4]
	$V[Cr(CN)_6]_{0.69}(SO_4)_{0.23}\cdot 3.0H_2O$	t_{2g}^3–t_{2g}^3/t_{2g}^2	315	[8]
$Cr^{III}Cr^{II}$	$[Cr_5(CN)_{12}]\cdot 10H_2O$	t_{2g}^3–$t_{2g}^3e_g^1$	240	[50]
$Mn^{II}V^{II}$	$(Et_4N)_{0.5}Mn_{1.25}[V(CN)_5]\cdot 2H_2O$	$t_{2g}^3e_g^2$–t_{2g}^3	230	[51]
$Cr^{III}Cr^{II}$	$Cs_{2/3}Cr[Cr(CN)_6]_{8/9}\cdot 4.4H_2O$[b]	t_{2g}^3–$t_{2g}^3e_g^1$	190	[50]
$V^{II}Mn^{II}$	$Cs^2Mn[V(CN)_6]$	t_{2g}^3–$t_{2g}^3e_g^2$	125	[51]
$Cr^{III}V^{IV}$	$(VO)[Cr(CN)_6]_{2/3}\cdot 3.3H_2O$	t_{2g}^3–t_{2g}^1	115	[52]
$Cr^{III}Mn^{II}$	$CsMn[Cr(CN)_6]$	t_{2g}^3–$t_{2g}^3e_g^2$	90	[53]
	$(NMe_4)Mn[Cr(CN)_6]$	t_{2g}^3–$t_{2g}^3e_g^2$	59	[54]
$Mn^{IV}Mn^{II}$	$Mn[Mn(CN)_6]\cdot 1.14H_2O$	t_{2g}^3–$t_{2g}^3e_g^2$	49	[55,56]
$Co^{II}Co^{II}$	$Co_3[Co(CN)_5]_2\cdot 8H_2O$	$t_{2g}^6e_g^1$–$t_{2g}^5e_g^2$	38	[57]
$Mn^{II}Mn^{II}$	$K_2Mn[Mn(CN)_6]$	t_{2g}^5–$t_{2g}^3e_g^2$	41	[58]
$Mn^{III}Mn^{II}$	$CsMn[Mn(CN)_6]\cdot 0.5H_2O$	t_{2g}^4–$t_{2g}^3e_g^2$	41	[58]
	$(NMe_4)[Mn_2(CN)_6]$	t_{2g}^4–$t_{2g}^3e_g^2$	28	[54]
$Mn^{II}Mn^{III}$	$Mn_3[Mn(CN)_6]_2\cdot 12H_2O$	t_{2g}^5–$t_{2g}^3e_g^1$	37	[58]
	$Mn_3[Mn(CN)_6]_2\cdot 12H_2O\cdot 1.7CH_3OH$	$t_{2g}^3e_g^2$–t_{2g}^4	29	[59]
$Mn^{III}Mn^{III}$	$Mn[Mn(CN)_6]$	t_{2g}^4–$t_{2g}^3e_g^1$	31	[56]
$Mn^{III}V^{III}$	$V[Mn(CN)_6]$	t_{2g}^4–t_{2g}^2	28	[56]
$Mn^{III}Cr^{III}$	$Cr[Mn(CN)_6]$	t_{2g}^4–t_{2g}^3	22	[56]
$Fe^{III}Co^{II}$	$Co_3[Fe(CN)_6]_2$	t_{2g}^5–$t_{2g}^5e_g^2$	14	[60]
$Fe^{III}Mn^{II}$	$Mn_3[Fe(CN)_6]_2$	t_{2g}^5–$t_{2g}^3e_g^2$	9	[61]
$Fe^{III}Fe^{II}$	$Fe_4[Fe(CN)_6]_3\cdot xH_2O$	t_{2g}^5–$t_{2g}^4e_g^2$	6[c]	[62]
$Fe^{III}Ni^{II}$	$Ni_3[Fe(CN)_6]_2$	t_{2g}^5–$t_{2g}^6e_g^2$	24[c]	[60]
$Mn^{III}Ni^{II}$	$Ni_3[Mn(CN)_6]_2\cdot 12H_2O$	t_{2g}^4–$t_{2g}^6e_g^2$	30[c]	[63]
	$CsNi[Mn(CN)_6]\cdot H_2O$	t_{2g}^4–$t_{2g}^6e_g^2$	42[c]	[63]
$Cr^{III}Ni^{II}$	$Ni_3[Cr(CN)_6]_2\cdot 9H_2O$	t_{2g}^3–$t_{2g}^6e_g^2$	60[c]	[63,64]
	$CsNi[Cr(CN)_6]\cdot 2H_2O$	t_{2g}^3–$t_{2g}^6e_g^2$	90[c]	[64]

[a] Although this compound is formulated as stoichiometric, a certain amount of V^{III} is present that is responsible for its ferrimagnetic behavior. [b] Or $Cs_6Cr_9[Cr(CN)_6]_8\cdot 40H_2O$. [c] The critical temperature in those cases corresponds to a ferromagnetic state, at difference with other compounds in which it corresponds to ferrimagnetic ordering.

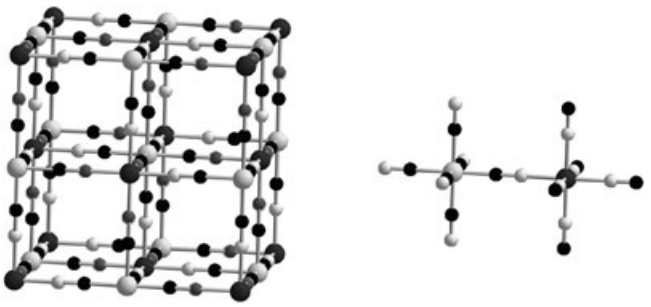

Figure 1. Ideal lattice corresponding to a Prussian-blue analogue (left) and molecular model extracted from the periodic lattice (right). In the ligands, the black spheres correspond to carbon, white spheres to nitrogen atoms.

two metallic sites M and M′ with different local spins, combined with an optimized number of unpaired electrons. We suggest that this goal can be sensibly achieved by means of a) calculations of J values on model complexes, using the nowadays standard computational techniques[22–25] that have been successfully applied to a variety of di- and polynuclear transition-metal complexes (see the Computational Details section), b) using the molecular mean field model to evaluate T_C from $|J|$. To compute the nearest neighbor coupling constant J, we use model dinuclear complexes $[(NC)_5M\text{-}CN\text{-}M'(NC)_5]^{n-}$ (Figure 1, right), coincident with the models previously used by Nishino et al.,[15,16] or their protonated analogues $[(HNC)_5M\text{-}CN\text{-}M'(NCH)_5]^{m+}$. Previous studies on dinuclear models showed[26] that the experimental behavior is intermediate between those calculated for molecular models with unprotonated and protonated bridging ligands. The different model molecules studied below have been chosen 1) to check that the calculations reproduce the experimental trends in the J values; 2) to gain new insights into the general behavior of this family of compounds and 3) to make predictions about new Prussian blue analogues that should present higher magnetic ordering temperatures and yet unprepared. The following groups of compounds will be discussed: a) Compounds with t_{2g}^3 and t_{2g}^3 electron configurations at the two metal atoms, antiferromagnetically coupled, that could yield high-temperature $M'[M(CN)_6]_x$ ($x<1$) magnets; b) potential ferrimagnetic systems formed by metal ions with electron configurations t_{2g}^m and t_{2g}^n that favor antiferromagnetic nearest-neighbor coupling, resulting in net magnetization for compounds with the $M'[M(CN)_6]$ stoichiometry; c) compounds with electron configurations that produce ferromagnetic coupling. The comparison of these three sets of calculations should allow us to evaluate possible strategies for the design of new high T_C Prussian blue magnets.

From electronic structure calculations on a dinuclear model we can obtain the coupling constant J, but not the Curie temperature. Instead, we use the approximate mean-field expression derived from Langevin, Weiss, and Néel [Eq. (1)],[27,28] which provides a bridge between the experimentally determined T_C and the computable exchange coupling constant between nearest M and M′ neighbors, J.

$$T_C = \frac{\sqrt{Z_M Z_{M'}}|J|\sqrt{xS_M(S_M+1)S_{M'}\ (S_{M'}+1)}}{3\,k_B} \qquad (1)$$

Here S_M and $S_{M'}$ are the local spins on centers M and M′, Z_M and $Z_{M'}$ the number of nearest neighbors of each type of metal atom and x corresponds to the stoichiometry of the $M'[M(CN)_6]_x$ compound. Although Equation (1) qualitatively indicates the fact that systems with stronger exchange coupling have higher ordering temperatures for a given stoichiometry, the T_C values obtained from calculated coupling constants in dinuclear models are significantly higher than the experimental ones. This overestimation of the T_C value is a well-known problem.[29] To obtain a rough estimate of the T_C values from our calculated exchange-coupling constants, we will scale the values by a constant factor that reproduces the experimental ordering temperature of $V[Cr(CN)_6]_{0.86}\cdot 2.8\,H_2O$, taking $x=2/3$, $Z_M=6$ and $Z_{M'}=4$.

Computational Details

The computational strategy adopted in previous theoretical studies on exchange-coupled dinuclear complexes has been applied here.[30] The J values are obtained by using Equation (2), where S_1 and S_2 are the total spins of the paramagnetic centers and $S_1>S_2$ has been assumed for heterodinuclear complexes.

$$E_{HS}-E_{LS} = -(2S_1S_2+S_2)J \qquad (2)$$

E_{HS} is the energy for the highest spin state and E_{LS} that of the state having the two metals with opposite spins (antiferromagnetic coupling). This expression is obtained without performing a spin-projection of the energy of the low-spin state. We adopt such an approach because the non-spin-projected results are systematically in better agreement with experimental data, a fact that can be attributed to the inclusion of nondynamic correlation effects in commonly used exchange functionals, due to the presence of the self-interaction error. If spin projection is applied to such density functional calculations, then a cancellation or a double counting of such effects results, as discussed recently by Polo et al.[31] The hybrid B3LYP method[32–34] has been used in all calculations as implemented in Gaussian98 (version A.11).[35] Owing to the complexity of the electronic structure of the studied compounds, we have employed the Jaguar code (version 4.1)[36] to generate an appropriate initial wavefunction, since it provides a better control of the local spin and multiplicities of the atoms. To maintain the electronic structure during the SCF procedure the quadratic convergence option must be employed. In all calculations, a triple-ζ basis set proposed by Ahlrichs et al.[37] was used for the transition-metal atoms, which included two extra p polarization functions, whereas the double-ζ basis set proposed by the same authors was used for all other atoms.[38] For the calculations containing the molybdenum atoms we have employed Stoll–Preuss quasi-relativistic pseudopotentials.[39]

To verify the effect of the modeling of the three-dimensional structure with a dinuclear molecule (Figure 1), we have calculated the J value for different models and basis sets in the case of $Cr^{III}Ni^{II}$ dinuclear compounds (Table 2). All the calculated values correctly reproduce the ferromagnetic character of the interaction found experimentally for the extended $Cr^{III}Ni^{II}$ compounds (Table 1, last two entries) and molecular systems.[40,41] In what follows, we will employ the $[(HNC)_5M\text{-}CN\text{-}M'(NCH)_5]^{4+}$ model for all the metal pairs analyzed, in which the protons attached to the cyano groups simulate the missing metal atoms of the extended structure and decrease the overall negative charge. For the most interesting cases, we will also report the calculations with the $[(NC)_5M\text{-}CN\text{-}M'(NC)_5]^{6-}$ model to calibrate the effect that the choice of the dinuclear model has on the calculated J value. The following bond lengths were used for the calculations: M–C 2.07, Mo–C 2.17, M′–N 2.10, Mo–N 2.20, C–N 1.13, C–H 1.0, and N–H 1.0 Å.

Table 2. Calculated J values[a] using the B3LYP functional for different molecular models of the $Cr^{III}Ni^{II}$ compound.

Model	J [cm^{-1}][b]
$[(NC)_5Cr\text{-}CN\text{-}Ni(NC)_5]^{6-}$	+22.4 (+16.2)
$[(HNC)_5Cr\text{-}CN\text{-}Ni(NCH)_5]^{4+}$	+27.9 (+19.7)
$[(NC)_5Cr\text{-}CN\text{-}Ni(NH_3)_5]^{-}$	+12.9 (+8.6)

[a] Ahlrich's basis set used. [b] The values in parenthesis were calculated with the basis set used in the work of Nishino et al.[14]

Results and Discussion

The results of our calculations on the molecular models with several combinations of transition metals are collected in Table 3. We have focused mostly on early transition metals

Table 3. Exchange-coupling constants J for the molecular models $[(HNC)_5M\text{-}CN\text{-}M'(NCH)_5]^{n+}$, and some examples with the $[(NC)_5M\text{-}CN\text{-}M'(NC)_5]^{n-}$ model (J' values), calculated with the B3LYP functional.

M, M′	Configuration	J [cm^{-1}]	J' [cm^{-1}]
$Mn^{III}V^{II}$	t_{2g}^4–t_{2g}^3	−503	−283
$Mo^{III}V^{II}$	t_{2g}^3–t_{2g}^3	−422	−358
$Cr^{III}Mo^{II}$	t_{2g}^3–t_{2g}^4	−372	−194
$V^{III}V^{II}$	t_{2g}^2–t_{2g}^3	−360	−270
$Cr^{III}V^{II}$	t_{2g}^3–t_{2g}^3	−241	−150
$Mo^{III}Cr^{II}$	t_{2g}^3–$t_{2g}^3e_g^1$	−186	
$Mn^{III}Cr^{II}$	t_{2g}^4–$t_{2g}^3e_g^1$	−122	
$Cr^{III}V^{IV}O$	t_{2g}^3–t_{2g}^1	−101	
$V^{III}V^{III}$	t_{2g}^2–t_{2g}^2	−99	
$V^{II}V^{II}$	t_{2g}^3–t_{2g}^3	−86	
$Cr^{III}Cr^{II}$	t_{2g}^3–$t_{2g}^3e_g^1$	−70	
$Mo^{III}Cr^{III}$	t_{2g}^3–t_{2g}^3	−63	
$Cr^{III}V^{III}$	t_{2g}^3–t_{2g}^2	−56	
$Mo^{III}V^{III}$	t_{2g}^3–t_{2g}^2	−52	
$Mn^{IV}Cr^{III}$	t_{2g}^3–t_{2g}^3	−33	
$Mn^{III}V^{III}$	t_{2g}^4–t_{2g}^2	−31	
$Cr^{III}Cr^{III}$	t_{2g}^3–t_{2g}^3	−29	
$V^{II}Mn^{II}$	t_{2g}^3–$t_{2g}^3e_g^2$	−23	
$Cr^{III}Mn^{II}$	t_{2g}^3–$t_{2g}^3e_g^2$	−18	
$V^{III}Ni^{II}$	t_{2g}^2–$t_{2g}^6e_g^2$	+24	
$Cr^{III}Ni^{II}$	t_{2g}^3–$t_{2g}^6e_g^2$	+28	
$Ti^{III}Cr^{III}$	t_{2g}^1–t_{2g}^3	+37	
$Mn^{IV}Ni^{II}$	t_{2g}^3–$t_{2g}^6e_g^2$	+121	
$Ti^{III}V^{II}$	t_{2g}^1–t_{2g}^3	+161	

because they have unpaired electrons in the t_{2g} orbitals that are appropriate for the interaction with the π system of the cyanide bridging ligands. Although T_C values estimated from the calculated coupling constants of dinuclear models are overestimated, as pointed out previously by Nishino et al,[15,16] we compare the calculated J values with those obtained from experimental T_C values by using Equation (1) to check if the computational results allow us to establish significant qualitative trends for the experimental behavior (Figure 2). It can be seen that a good correlation exists between the experimentally derived and the theoretical coupling constant, even if the correlation is not linear. In any event, it becomes clear that a calculated antiferromagnetic coupling stronger than that obtained for the $Cr^{III}V^{II}$ model ($J = -241$ cm^{-1}) should imply a T_C value above room temperature for the corresponding extended solid, other things being equal (i.e., local spins and number of nearest neighbors). The main observations that can be made from the results of our calculations (Table 3) together with the analysis of the experimental data (Table 1) are summarized as follows:

1) Four metal pairs present stronger antiferromagnetic coupling than the Cr^{III}–V^{II} couple. These are: Mn^{III}–V^{II}, Mo^{III}–V^{II}, Cr^{III}–Mo^{II} and V^{III}–V^{II}. For such systems, we have also performed the calculations with the unprotoned model to verify this assumption.
2) The electron configuration of M and M′ affects the nature and magnitude of the coupling in predictable ways, with t_{2g}^m–t_{2g}^n pairs giving strong antiferromagnetic interactions (with the exception of the Ti^{III} compounds, see below), t_{2g}^m–$t_{2g}^n e_g$ or t_{2g}^m–$t_{2g}^n e_g^2$ pairs weaker antiferromagnetic interactions and t_{2g}^m–$t_{2g}^6 e_g^2$ pairs yielding ferromagnetic coupling.
3) The metal ions in the M′ site that give strongest antiferromagnetic coupling are V^{II}, Cr^{II}, and Mo^{II}.
4) Mo^{III} at the M site systematically gives stronger antiferromagnetic coupling than the Cr^{III} analogues.
5) The magnitude of the coupling for analogous pairs of electron configurations is strongly affected by the oxidation state of the metal atoms. In particular, for the t_{2g}^3–t_{2g}^3 pairs, a significantly stronger antiferromagnetic coupling appears for M^{III} and M'^{II} pairs.
6) Models with Ti^{III} in the M site are in all cases predicted to be ferromagnetic, even when coupled with a t_{2g}^3 metal ion at the M′ site.
7) The results for the models with Mn^{II} in the M′ site reproduce correctly the trend of the experimental data, giving a slightly stronger antiferromagnetic coupling for the V^{II} compounds than for the Cr^{III} one.

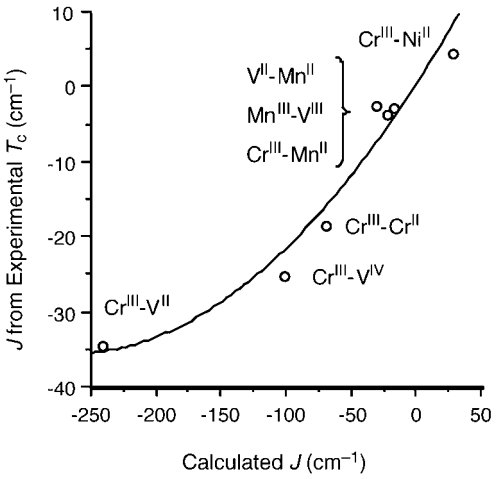

Figure 2. Relationship between calculated exchange coupling constants for dinuclear model complexes (Table 3) and coupling constants for extended solids estimated from the experimental T_C values (Table 1) through Equation (1).

Let us now discuss in more detail some of these results. Among metal pairs for which the strongest antiferromagnetic coupling is predicted we find Mn^{III}–V^{II}, V^{III}–V^{II}, and Mo^{III}–V^{II}. In the related experimentally characterized Prussian blue analogues, the stoichiometry is $M_2V^{II}{}_3$, for which a ferrimagnetic behavior is expected and the ordering temperature should then be above room temperature. To obtain a rough idea of the meaning of the calculated exchange coupling constants in terms of the experimentally determinable T_C values, we have calculated from Equation (1) the order-

ing temperatures for the most strongly coupled dinuclear models, with a scaling factor such that the value estimated for $V[Cr(CN)_6]_{0.86}\cdot 2.8H_2O$ coincides with the experimental one (Table 1). We thus obtain T_C values above room temperature for several $M^{III}M'^{II}$ couples (Table 4). It is noteworthy

Table 4. Curie temperatures for Prussian blue analogues with the stoichiometry $M_3^{II}[M^{III}(CN)_6]_2$, estimated from the calculated coupling constants J for the molecular models $[(HNC)_5M\text{-}CN\text{-}M'(NCH)_5]^{n+}$.

M, M′	Configuration	T_C [K]
$Mn^{III}V^{II}$	t_{2g}^4–t_{2g}^3	480
$Mo^{III}V^{II}$	t_{2g}^3–t_{2g}^3	552
$Cr^{III}Mo^{II}$	t_{2g}^3–t_{2g}^4	355
$V^{III}V^{II}$	t_{2g}^2–t_{2g}^3	344
$Cr^{III}V^{II}$	t_{2g}^3–t_{2g}^3	315
$Cr^{III}Mo^{II}$	t_{2g}^3–t_{2g}^4	185
$Mo^{III}Cr^{II}$	t_{2g}^3–$t_{2g}^3e_g^1$	308
$Mn^{III}Cr^{II}$	t_{2g}^4–$t_{2g}^3e_g^1$	147
$Cr^{III}Cr^{II}$	t_{2g}^3–$t_{2g}^3e_g^1$	116
$Cr^{III}Mn^{II}$	t_{2g}^3–$t_{2g}^3e_g^2$	36

that in these cases the expected magnetic ordering temperature is not only above room temperature, but higher than in the previously known Prussian blue magnets and probably higher than the decomposition temperature. Although the $Mo^{III}V^{II}$ Prussian blue may seem unlikely because the Mo^{III} cation appears usually with coordination number higher than six, Beauvais et al. have recently synthesized a dinuclear $[Mo_2(CN)_{11}]^{5-}$ complex with octahedral coordination of the metal atoms and a J value of $-226\,cm^{-1}$,[42] thus suggesting that the type of compound proposed here should be obtainable. The systems containing Mo^{III} ions show larger exchange coupling constants than the equivalent compounds with first transition series elements due to the more diffuse character of the 4d orbitals in comparison with the 3d ones, as verified in a recent computational study.[43]

Among the interactions between t_{2g}^m and t_{2g}^n configurations a few cases deserve a more detailed discussion. The fact that the t_{2g}^3–t_{2g}^2 (Cr^{III}–V^{III} and Mo^{III}–V^{III}) and t_{2g}^2–t_{2g}^3 pairs (V^{III}–V^{II}) present antiferromagnetic coupling of quite different strengths ($|J|\approx 50$ and $360\,cm^{-1}$, respectively) might be attributed to the strong asymmetry of the CN bridge, but in the light of the strong influence that the oxidation state has on the coupling constants for other configurations, it is more likely that it is the choice of metals and oxidation states that produces such a remarkable difference (see point 5 above). Also the apparent disagreement between the low experimental T_C in the Mn^{III}–Cr^{III} couple and the high negative J value calculated for the related Mn^{III}–V^{II} pair with the same configuration (t_{2g}^4–t_{2g}^3) should be attributed to the different choices of oxidation states in the two cases. An interesting possibility is provided by a t_{2g}^3–t_{2g}^4 couple, for which a strong antiferromagnetic coupling is expected, similar to that found for the t_{2g}^3–t_{2g}^2 pairs, but that is unlikely for first row transition metals in the M′ site since the N donor atoms favor the high spin $t_{2g}^3e_g^1$ configuration rather than the low spin t_{2g}^4 one. However, the t_{2g}^3–t_{2g}^4 situation should be possible by using a second- or third-row transition metal at the M′ site, and our calculations on the Cr^{III}–Mo^{II} compound confirm this idea.

It is not easy to find a simple general explanation for the large range covered by the experimental (Table 1) and calculated (Table 3) coupling constants. One of the usual ways of rationalizing the exchange coupling between two unpaired electrons makes use of the relationships between J and the overlap integral between the two localized (or "magnetic") orbitals bearing such electrons, devised by Kahn and Briat[11] and by Noodlemann.[44] A unified view of these models has been presented recently by Mouesca.[45] Focusing on the Noodlemann approach that involves broken-symmetry solutions, the aforementioned relationship is given by Equation (3) where k' is a ferromagnetic contribution (associated only with t_{2g}–e_g interactions), U is the on-site interelectron repulsion that results from transferring an electron from one metal to another and S_{ab} is the overlap integral between a pair of magnetic orbitals a (centered at M) and b (centered at M′).

$$J = 2k' - US_{ab}^2 \tag{3}$$

For such a simple system, we and other authors[30,46] have shown that the overlap between the magnetic orbitals can be approximately calculated from the spin population of the transition metal atoms. Thus, for a symmetric homodinuclear complex with one unpaired electron at each metal atom the simple expression (4) results, where a and b are the localized molecular orbitals, whereas ρ_T and ρ_{BS} are the spin population at the metal atoms in the triplet and broken-symmetry states, respectively.[30]

$$S_{ab}^2 = \langle a|b\rangle^2 \approx \rho_T^2 - \rho_{BS}^2 \tag{4}$$

In the appendix we propose that, assuming that the exchange coupling constant can be expanded as a sum of squares of overlap integrals S_{ab} between the non-orthogonal pairs of localized orbitals, the relationship between J and the overlap integral ([Eq. (3)]) can be approximately found to be proportional to a function of the calculated spin densities at the metal atoms, Δ ([Eq. (5)]). Here ρ_{HS1} and ρ_{HS2} are the spin populations at the metal atoms M and M′ in the high-spin state, whereas ρ_{LS1} and ρ_{LS2} are the corresponding populations in the low-spin state.

$$J \propto \Delta = [(\rho_{HS1}^2 - \rho_{LS1}^2)^{1/2} + (\rho_{HS2}^2 - \rho_{LS2}^2)^{1/2}]^2 \tag{5}$$

When the coupling constants calculated here are plotted as a function of the corresponding Δ values, a fair correlation appears (Figure 3). Deviations from the general trend may be attributed to the differences in electron configuration, oxidation state and transition series of the metal ions present, which should be reflected in differences in the k' and U parameters in Equation (3). This observation is confirmed by analyzing the family of complexes with the same electron configurations (t_{2g}^3–t_{2g}^3), represented by black

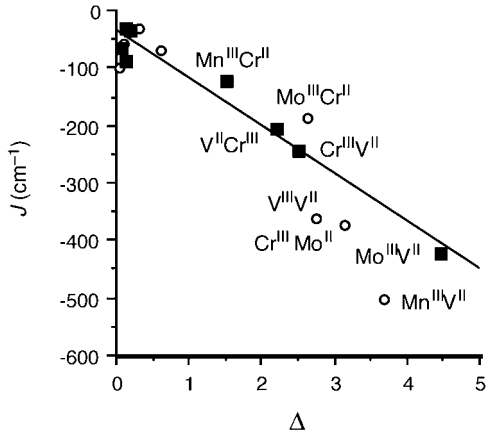

Figure 3. Calculated exchange coupling constants (Table 3) represented as a function Δ of the Mulliken spin populations of the metal atoms in the high- and low-spin states ([Eq. (5)]) of dinuclear complexes with t_{2g}^{m}–t_{2g}^{n} electron configurations. The squares correspond to those complexes with t_{2g}^{3}–t_{2g}^{3} configuration and the line is a least-squares fitting for those points only.

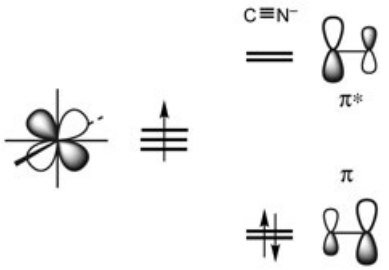

Scheme 1.

squares in Figure 3, for which a nice linear correlation is found.

A result that should be of interest for the design of new magnetic Prussian blue analogues is the strong dependence of the exchange coupling constant on the oxidation state of the two metal atoms. If we focus only on the t_{2g}^{m}–t_{2g}^{n} couples, for which no ferromagnetic t_{2g}–e_g contributions exist, we can see in Figure 3 that all complexes with strong antiferromagnetic coupling ($-503 < J < -122\ cm^{-1}$) correspond to metal pairs in oxidation states III–II, irrespective of the number of t_{2g} unpaired electrons. In contrast, if we consider those pairs in which the two first row metal atoms have the same oxidation state (with the exception of Ti compounds, to be discussed below): V^{III}–V^{III}, V^{II}–V^{II}, Cr^{III}–V^{III}, Mn^{III}–V^{III}, and Cr^{III}–Cr^{III}, we observe weaker calculated J values (between -29 and $-99\ cm^{-1}$, Table 3).

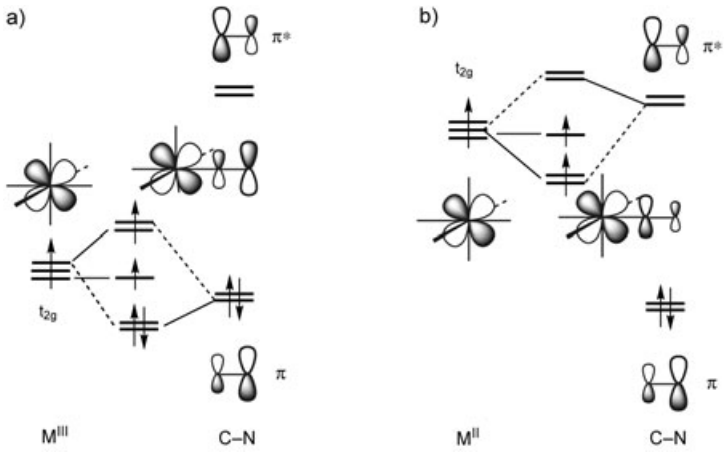

Scheme 2.

The strong dependence of J on the oxidation state of the metals can be rationalized by analyzing the composition of the Kohn–Sham orbitals of the broken-symmetry solution, taking into account the relationship between the overlap integral and J ([Eq. (3)]). We will first show how the localization of the magnetic orbitals changes with the oxidation state of the two metal sites, and then interpret the effect on the exchange coupling according to overlap criteria. We start by assuming that the metal t_{2g} orbitals appear in the energy scale somewhere in-between the π and π* orbitals of the bridging cyanide, consistent with the fact that the unpaired electrons are metal-centered (Scheme 1). Depending on the metal oxidation state, the d electrons experience different attraction by the net charge of the atomic core and the energy of the d orbitals decreases with increasing oxidation state. Since one of the key factors that determines the magnitude of the interaction between two orbitals is their being similar in energy, we should expect metals in high oxidation states to interact preferentially with the π orbital of cyanide and those in low oxidation states to interact mostly with π*, as depicted in Scheme 2 a and b, respectively. The present results indicate that the effect of the metal oxidation state on the d orbital energy is more important than that of the nuclear charge, which is less effective due to screening by the core electrons. If we consider systems with the same combination of oxidation states the exchange coupling is in most cases stronger for a metal with smaller atomic number, although then also the electron configuration changes and it is not straightforward to ascribe such effect to one of these two factors. This orbital energy scheme is in agreement with the well-established dependence of atomic orbital energies on the atomic number[47] and charge.[48]

In a cyano-bridged heterodinuclear compound the t_{2g} orbitals of the two metal atoms interact with the π system of the bridge, giving highly localized magnetic orbitals with contribution at the bridging atoms, as illustrated in Scheme 3. To have a large overlap between these, hence strong antiferromagnetic coupling, we must have the largest

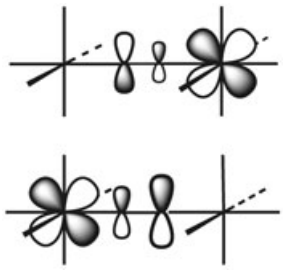

Scheme 3.

possible contribution at the bridge in both magnetic orbitals. This is most efficiently done if one metal interacts mostly with the π, the other with the π* orbital, that is, if the oxidation states of the two metal atoms are different. Our results suggest that fine tuning of the metal orbital energies results in the best choice for a trivalent and a divalent metal atom. However, if the orbital picture presented here is correct, we should expect the two combinations M^{III}–M'^{II} and M^{II}–M'^{III} to give similarly strong coupling. Since in all our calculations the high-oxidation-state metal was at the C_6 site and the low oxidation state one at the N_6 site, we tested such a prediction by calculating the V^{II}–Cr^{III} complex, for which we also find a larger coupling constant ($-204\ cm^{-1}$, to be compared with $-241\ cm^{-1}$ for the Cr^{III}–V^{II} pair) than for metal combinations with the same oxidation state. The fact that only two of the three t_{2g} orbitals of each metal atom interact with the bridge may explain the minute differences in exchange-coupling constants found between, for example, the t_{2g}^3–t_{2g}^3 and t_{2g}^3–t_{2g}^2 pairs in compounds with the same combination of oxidation states (see above).

An intriguing result of our calculations is the ferromagnetic interaction predicted for compounds with Ti^{III} at the M site, in apparent disagreement with the usual expectation of antiferromagnetic coupling between t_{2g} electrons. Such a result, however, can be easily understood if we take into account the real symmetry of the dinuclear [$(NC)_5$-Ti-CN-M′-$(NC)_5$] models used in our calculations, C_{4v}, in which the symmetry axis z is coincident with the Ti-CN-M′ skeleton. In that point group, the xy orbital belongs to the B_2 symmetry representation, whereas the xz and yz orbitals are degenerate, of E symmetry. In our model dinuclear compounds, the Ti orbital bearing the unpaired electron (b_2, or xy) happens to be of δ symmetry relative to the Ti–C bond (Scheme 4a) and is therefore forbidden by symmetry to interact with the d orbitals of M′ through the bridge π orbitals (e). Therefore, according to the orbital models of magnetic exchange interactions, electrons in non-interacting orbitals can only yield ferromagnetic coupling. Similar considerations allow us to explain why the antiferromagnetic coupling for, for example, the $V^{III}V^{II}$ pair with t_{2g}^2–t_{2g}^3 configuration (i.e., e^2–e^2b_2 in the C_{4v} point group) is stronger than for the t_{2g}^3–t_{2g}^3 (e^2b_2)–(e^2b_2) $Cr^{III}V^{II}$ pair, since two ferromagnetic contributions (e–b_2 and b_2–e) are at work in the latter but only one (e-b_2) in the former case.

Coming back to the Ti^{III} systems, it is not obvious, though, why the electron configuration with the δ-type t_{2g} (b_2) orbital of Ti^{III} bearing the unpaired electron is the most stable one (our calculations indicate that it is $22.1\ kJ\,mol^{-1}$ more stable than the one with the unpaired electron in a π (e) orbital of the type shown in Scheme 4b). The analysis of the Kohn–Sham orbitals for the two configurations in the Ti^{III}–V^{II} compound suggests that strong localization of the δ orbital at the Ti site (Scheme 4a) results in negligible repulsion with the t_{2g} electrons localized at the V (M′) atom. In contrast, for the electron configuration in which the Ti unpaired electron resides in a π-type orbital, due to significant delocalization through the V atom (Scheme 4b), a much stronger interelectronic repulsion results. Such a behavior thus depends on the subtle interplay of one- and two-electron interactions, and experimental verification of the ferromagnetic behavior of Ti compounds such as those calculated here would be highly desirable to gain new insights into the unexpected subtleties of their exchange interactions.

From our orbital analysis it is clear that ferromagnetism in the model dinuclear Ti^{III}–Cr^{III} and Ti^{III}–V^{III} compounds arises as a result of their one-dimensional nature, since in 2D or 3D cyano-bridged networks the orbital depicted in Scheme 4a would interact with M′ atoms in the other two directions of space resulting in a non-negligible antiferromagnetic contribution to the exchange coupling. Does that mean that we cannot convert our prediction of strong ferromagnetism in these Ti^{III} compounds into a ferromagnetic extended structure of the Prussian blues family? On the contrary, the knowledge we have gained can be applied to designing a potentially ferromagnetic solid. To have ferromagnetism as in our dinuclear models we need to preserve the one-dimensional nature around the Ti atom, using as a building block a *trans*-dicyano complex (**1**) to form a network with a substitution-labile complex of M′. The choice of the Ti building block is not straightforward, since the room left for the

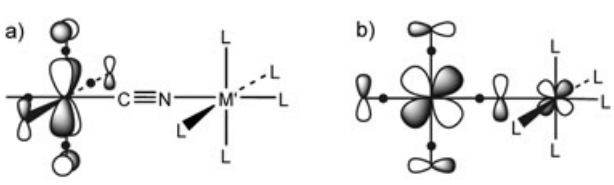

Scheme 4.

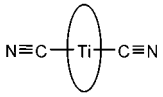

1

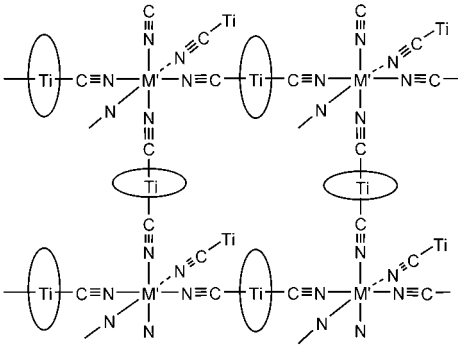

equatorial ligands of Ti is not large, but related buildings can be found as "super-Prussian blues".[49] The effect of spin-orbit coupling in Ti^{III} would add to the complexity of their magnetic behavior, but the expected novel properties of such a material are worthy of some synthetic effort.

Conclusion

The goal of this work was to search for new compounds of the Prussian blue family that could be expected to present magnetic ordering at room temperature and to establish the factors that control the exchange coupling in such systems. To that end we have carried out a theoretical study of the exchange-coupling constants in a variety of dinuclear molecular models formed by the basic building blocks of the Prussian blues. Since there is a direct relationship between the ordering temperature and the exchange coupling constant, the calculated J values should provide reasonable qualitative hints on the expected ordering temperatures of the new compounds.

We distinguish three subclasses of Prussian blue analogues: a) Compounds with significant ferromagnetic coupling between the two metals. b) Compounds with strong antiferromagnetic coupling between two metals bearing the same local spin, that become ferrimagnetic when the M:M′ stoichiometry is different from 1:1. c) Compounds with strong antiferromagnetic coupling between two metals with different spins, leading to ferrimagnetism.

As for the subclass of ferromagnetically coupled Prussian blues, a high T_C is expected for the $Mn^{IV}Ni^{II}$ pair due to the interaction between unpaired t_{2g} and e_g electrons. Besides, Ti^{III} at the C-bonded site has been found to be well suited to forming ferromagnetic systems, provided it forms only two *trans*-cyano bridges, with a particularly strong ferromagnetic coupling ($J = +161\ cm^{-1}$) predicted for a $Ti^{III}V^{II}$ pair. This behavior is counterintuitive, according to the prevailing orbital rules, and represents a novel phenomenon.

The second and third subclasses have in common the antiferromagnetic interaction between nearest-neighbors. The factors that favor strong antiferromagnetic interactions are: 1) Second- or third-row transition metals give stronger coupling than first row ones. 2) The appropriate electron configurations for the two metals are the t_{2g}^{m}–t_{2g}^{n} ones. 3) Antiferromagnetic coupling is strongly favored by having the C-bonded metal atom in the +3 oxidation state and the N-bonded metal in the +2 oxidation state or vice versa. 4) The strength of the exchange coupling between t_{2g}^{m} and t_{2g}^{n} metals through a cyanide bridge is seen to be roughly correlated to a simple expression of the atomic spin populations calculated at the metal atoms. According to these results, among the subclass of ferrimagnetic compounds with the oxidation states $M^{III}M'^{II}$, improved ordering temperatures over the existing $Cr^{III}V^{II}$ system ($T_C = 315$ K, our calculated $J = -241\ cm^{-1}$) are to be expected for the following pairs of metal ions: $Mo^{III}V^{II}$ (estimated $T_C \approx 552$ K), $Cr^{III}Mo^{II}$ ($T_C \approx 355$ K), $Mn^{III}V^{II}$ ($T_C \approx 480$ K), and $V^{III}V^{II}$ ($T_C \approx 344$ K).

Appendix

Relationship between exchange-coupling constant and overlap: We focus here on dinuclear systems bearing three unpaired electrons in t_{2g} orbitals of transition metal atoms, for which we can disregard the overlap between the δ orbitals perpendicular to the bridging cyanide. Thus, we consider the two localized molecular orbitals of π symmetry a and a', mostly localized at one metal center (i.e., d_{xz} and d_{yz}), and the corresponding orbitals b and b' localized at the second metal atom. Such molecular orbitals for a nonsymmetric dinuclear complex are built up from atomic orbitals at the two metal centers (χ_1, χ_2, χ'_1, χ'_2), and linear combinations of the two degenerate π-type orbitals of the bridging ligand, φ_1, φ'_1, φ_2, and φ'_2 [see (A1)–(A4)].

$$a = \alpha_1\chi_1 + \beta_2\chi_2 + \gamma_1\varphi_1 \tag{A1}$$

$$a' = \alpha_1\chi'_1 + \beta_2\chi'_2 + \gamma_1\varphi'_1 \tag{A2}$$

$$b = \beta_1\chi_1 + \alpha_2\chi_2 + \gamma_2\varphi_2 \tag{A3}$$

$$b' = \beta_1\chi'_1 + \alpha_2\chi'_2 + \gamma_2\varphi'_2 \tag{A4}$$

Furthermore, the following non-diagonal overlap integrals are strictly orthogonal, since they correspond to orbitals that are rotated by 90° relative to each other around the M-C-N-M′ axis [see (A5)].

$$\langle a|b'\rangle = \langle a'|b\rangle = 0 \tag{A5}$$

The overlap integral between the molecular orbitals can then be written as expression (A6).

$$\begin{aligned}\langle a|b\rangle = \langle a'|b'\rangle =& \alpha_1\beta_1 + \alpha_2\beta_2 + \gamma_1\gamma_2\langle\varphi_1|\varphi_2\rangle + \\ & (\alpha_1\alpha_2 + \beta_1\beta_2)\langle\chi_1|\chi_2\rangle + \gamma_1[\beta_1\langle\chi_1|\varphi_1\rangle + \alpha_2\langle\chi_2|\varphi_1\rangle] + \\ & \gamma_2[\alpha_1\langle\chi_1|\varphi_2\rangle + \beta_2\langle\chi_2|\varphi_2\rangle]\end{aligned} \tag{A6}$$

Assuming significant localization of the orbitals at the metal centers (i.e., $\alpha_1, \alpha_2 \gg \beta_1, \beta_2, \gamma_1, \gamma_2$), we can neglect in a first approximation the terms with coefficients such as $\beta_1\beta_2$, $\gamma_1\gamma_2$ and $\beta_i\gamma_j$, as well as the integrals involving cross-terms with the ligands′ orbitals, such as $\langle\chi_1|\varphi_2\rangle$. Furthermore, the direct overlap between the metal atomic orbitals can be neglected, $\langle\chi_1|\chi_2\rangle \approx 0$, given the long distance between the two metal atoms. As a result, the only significant overlap integrals between the magnetic orbitals can be approximated as expression (A7).

$$\langle a|b\rangle = \langle a'|b'\rangle \approx \alpha_1\beta_1 + \alpha_2\beta_2 \tag{A7}$$

On the other hand, the spin density at the metal atoms in the high- and low-spin solutions can be expressed following a Mulliken population analysis scheme. For the metal center M in the high-spin solution we have expression (A8).

$$\rho_{HS1} = 2\alpha_1^2 + 2\beta_1^2 + (\alpha_1\beta_2 + \alpha_2\beta_1)\langle\chi_1|\chi_2\rangle + (\alpha_1\beta_2 + \alpha_2\beta_1)\langle\chi_1'|\chi_2'\rangle + \gamma_1\alpha_1(\langle\chi_1|\varphi_1\rangle + \langle\chi_1'|\varphi_1'\rangle) + \gamma_2\beta_1(\langle\chi_1|\varphi_2\rangle + \langle\chi_1'|\varphi_2'\rangle) \quad \text{(A8)}$$

Expression (A8) that can be simplified by adopting the same approximations employed for the overlap integrals, resulting in expression (A9).

$$\rho_{HS1} \approx 2\alpha_1^2 + 2\beta_1^2 \quad \text{(A9)}$$

Proceeding in a similar way, it is possible to obtain the equivalent expressions (A10)–(A12) for the other spin populations at the metals.

$$\rho_{LS1} \approx 2\alpha_1^2 - 2\beta_1^2 \quad \text{(A10)}$$

$$\rho_{HS2} \approx 2\alpha_2^2 + 2\beta_2^2 \quad \text{(A11)}$$

$$\rho_{LS2} \approx 2\alpha_2^2 - 2\beta_2^2 \quad \text{(A12)}$$

Finally, the square of the overlap integrals between the localized molecular orbitals can be expressed from Equation (A7) as Equation (A13).

$$\langle a|b\rangle^2 + \langle a'|b'\rangle^2 \approx 2\alpha_1^2\beta_1^2 + 2\alpha_2^2\beta_2^2 + 4\alpha_1\beta_1\alpha_2\beta_2 \quad \text{(A13)}$$

By combining Equations (A9)–(A13), the sum of the overlap integrals can be expressed (A14) as a function of the atomic spin density at the metal atoms in the high and low spin solutions.

$$\langle a|b\rangle^2 + \langle a'|b'\rangle^2 \approx 8((\rho_{HS1}^2 - \rho_{LS1}^2)^{1/2} + (\rho_{HS2}^2 - \rho_{LS2}^2)^{1/2})^2 \quad \text{(A14)}$$

This expression was used to get Equation (5) and Figure 3.

Acknowledgement

Financial support to this work was provided by the Dirección General de Investigación (DGI) through project number BQU2002–04033-C02–01. Additional support from the Comissió Interdepartamental de Ciència i Tecnologia (CIRIT) through grant 2001SGR-0044 is also acknowledged. The computing resources employed in this work at CESCA/CEPBA have been made generously available through grants from CIRIT and the Universitat de Barcelona. The authors also thank ICREA for funding the stay of M. V. in Barcelona as a Visiting Researcher.

[1] O. Kahn, *Molecular Magnetism*, VCH Publishers, New York, **1993**.
[2] J. S. Miller, M. Drillon in *Magnetism: Molecules to Materials, vol. 1–4*, Wiley-VCH, Weinheim, **2001**–**2004**.
[3] J. M. Manriquez, G. T. Yee, R. S. McLean, A. J. Epstein, J. S. Miller, *Science* **1991**, *252*, 1415.
[4] S. Ferlay, T. Mallah, R. Ouahes, P. Veillet, M. Verdaguer, *Nature* **1995**, *378*, 701.
[5] O. Hatlevik, W. E. Buschmann, J. Zhang, J. L. Manson, J. S. Miller, *Adv. Mater.* **1999**, *11*, 914.
[6] S. M. Holmes, S. G. Girolami, *J. Am. Chem. Soc.* **1999**, *121*, 5593.
[7] R. Garde, F. Villain, M. Verdaguer, *J. Am. Chem. Soc.* **2002**, *124*, 10531.
[8] E. Dujardin, S. Ferlay, X. Phan, C. Desplanches, C. Cartier dit Moulin, P. Saintavict, F. Baudelet, E. Dartyge, P. Veillet, M. Verdaguer, *J. Am. Chem. Soc.* **1998**, *120*, 11347.
[9] M. Verdaguer, A. Bleuzen, C. Train, R. Garde, F. F. deBiani, C. Desplanches, *Philos. Trans. R. Soc. London Ser. A* **1999**, *357*, 2959.
[10] M. Verdaguer, A. Bleuzen, V. Marvaud, J. Vaissermann, M. Seuleiman, C. Desplanches, A. Scuiller, C. Train, R. Garde, G. Gelly, C. Lomenech, I. Rosenman, P. Veillet, C. Cartier, F. Villain, *Coord. Chem. Rev.* **1999**, *192*, 1023.
[11] O. Kahn, B. Briat, *J. Chem. Soc. Faraday Trans. 1* **1976**, *72*, 268.
[12] O. Kahn, B. Briat, *J. Chem. Soc. Faraday Trans. 1* **1976**, *72*, 1441.
[13] V. Eyert, B. Siberchicot, M. Verdaguer, *Phys. Rev. B* **1997**, *56*, 8959.
[14] N. M. Harrison, B. G. Searle, E. A. Seddon, *Chem. Phys. Lett.* **1997**, *266*, 507.
[15] M. Nishino, S. Takeda, W. Mori, A. Nakamura, K. Yamaguchi, *Synth. Met.* **1997**, *85*, 1763.
[16] M. Nishino, Y. Yoshioka, K. Yamaguchi, *Chem. Phys. Lett.* **1998**, *297*, 51.
[17] H. Weihe, H. U. Güdel, *Comments Inorg. Chem.* **2000**, *22*, 75.
[18] M. Verdaguer, A. Bleuzen, V. Marvaud, J. Vaissermann, F. Tournilhac, C. Train, R. Ouahes, R. Garde, F. Fabrizi De Biani, C. Desplanches, A. Scuiller in *Coordination Chemistry at the Turn of the Century*, *Vol. 4*, Slovak Technical University Press, Bratislava, **1997**, p. 67.
[19] A. V. Palli, B. S. Tsukerblat, M. Verdaguer, *J. Chem. Phys.* **2002**, *117*, 7896.
[20] V. S. Hendrickx, V. S. Mironov, L. F. Chibotaru, A. Ceulemans, *J. Am. Chem. Soc.* **2003**, *125*, 9750.
[21] L. F. Chibotaru, V. S. Mironov, A. Ceulemans, *Angew. Chem.* **2001**, *113*, 4561; *Angew. Chem. Int. Ed.* **2001**, *40*, 4429.
[22] E. Ruiz, P. Alemany, S. Alvarez, J. Cano, *J. Am. Chem. Soc.* **1997**, *119*, 1297.
[23] E. Ruiz, J. Cano, S. Alvarez, P. Alemany, *J. Am. Chem. Soc.* **1998**, *120*, 11122.
[24] E. Ruiz, S. Alvarez, A. Rodríguez-Fortea, P. Alemany, Y. Pouillon, C. Massobrio, in *Magnetism: Molecules to Materials*, *Vol. 2* (Eds.: J. S. Miller, M. Drillon), Wiley-VCH, Weinheim, **2001**, p. 227.
[25] C. Desplanches, E. Ruiz, A. Rodríguez-Fortea, S. Alvarez, *J. Am. Chem. Soc.* **2002**, *124*, 5197.
[26] B. Gillon, C. Mathonière, E. Ruiz, S. Alvarez, A. Cousson, O. Kahn, *J. Am. Chem. Soc.* **2002**, *124*, 14433.
[27] L. Néel, *Ann. Phys. (Paris)* **1948**, *3*, 137.
[28] A. Herpin, *Théorie du Magnétisme*, I. N. S. T. N., Saclay, **1968**.
[29] G. S. Rushbrook, P. J. Wood, *Mol. Phys.* **1958**, *1*, 257.
[30] E. Ruiz, J. Cano, S. Alvarez, P. Alemany, *J. Comput. Chem.* **1999**, *20*, 1391.
[31] V. Polo, E. Kraka, D. Cremer, *Theor. Chem. Acc.* **2002**, *107*, 291.
[32] C. Lee, W. Yang, R. G. Parr, *Phys. Rev. B* **1988**, *37*, 785.
[33] A. D. Becke, *Phys. Rev. A* **1988**, *38*, 3098.
[34] A. D. Becke, *J. Chem. Phys.* **1993**, *98*, 5648.
[35] M. J. Frisch, G. W. Trucks, H. B. Schlegel, G. E. Scuseria, M. A. Robb, J. R. Cheeseman, V. G. Zakrzewski, J. A. Montgomery, R. E. Stratmann, J. C. Burant, S. Dapprich, J. M. Millam, A. D. Daniels, K. N. Kudin, M. C. Strain, O. Farkas, J. Tomasi, V. Barone, M. Cossi, R. Cammi, B. Mennucci, C. Pomelli, C. Adamo, S. Clifford, J. Ochterski, G. A. Petersson, P. Y. Ayala, Q. Cui, K. Morokuma, D. K. Malick, A. D. Rabuck, K. Raghavachari, J. B. Foresman, J. Cioslowski, J. V. Ortiz, B. B. Stefanov, G. Liu, A. Liashenko, P. Piskorz, I. Komaromi, R. Gomperts, R. L. Martin, D. J. Fox, T. Keith, M. A. Al-Laham, C. Y. Peng, A. Nanayakkara, C. Gonzalez, M. Challacombe, P. M. W. Gill, B. G. Johnson, W. Chen, M. W. Wong, J. L. Andres, M. Head-Gordon, E. S. Replogle, J. A. Pople, Gaussian 98 (Revision A.11) ed., Gaussian, Inc, Pittsburgh, PA, **1998**.
[36] Jaguar 4.1, Schrödinger Inc., Portland, **2000**.
[37] A. Schaefer, C. Huber, R. Ahlrichs, *J. Chem. Phys.* **1994**, *100*, 5829.
[38] A. Schaefer, H. Horn, R. Ahlrichs, *J. Chem. Phys.* **1992**, *97*, 2571.
[39] D. Andrae, U. Häussermann, M. Dolg, H. Stoll, H. Preuss, *Theor. Chim. Acta* **1990**, *77*, 123.

[40] V. Marvaud, C. Decroix, A. Scuiller, C. Guyard-Duhayon, J. Vaissermann, F. Gonnet, M. Verdaguer, *Chem. Eur. J.* **2003**, *9*, 1677.
[41] V. Marvaud, C. Decroix, A. Scuiller, F. Tuyèras, C. Guyard-Duhayon, J. Vaissermann, J. Marrot, F. Gonnet, M. Verdaguer, *Chem. Eur. J.* **2003**, *9*, 1692.
[42] L. G. Beauvais, J. R. Long, *J. Am. Chem. Soc.* **2002**, *124*, 2110.
[43] C. Desplanches, E. Ruiz, S. Alvarez, *Eur. J. Inorg. Chem.* **2003**, 1756.
[44] L. Noodlemann, D. A. Case, *Adv. Inorg. Chem.* **1992**, *38*, 423.
[45] J. M. Mouesca, *J. Chem. Phys.* **2000**, *113*, 10505.
[46] R. Caballol, O. Castell, F. Illas, I. d. P. R. Moreira, J. P. Malrieu, *J. Phys. Chem. A* **1997**, *101*, 7860.
[47] A. Vela, J. L. Gázquez, *J. Phys. Chem.* **1988**, *92*, 5688.
[48] S. P. McGlynn, *Introduction to Applied Quantum Chemistry*, Holt, Rinehart and Winston, New York, **1972**.
[49] K. R. Dunbar, R. A. Heintz, *Prog. Inorg. Chem.* **1997**, *45*, 283.
[50] T. Mallah, S. Thiébaut, M. Verdaguer, P. Veillet, *Science* **1993**, *262*, 1554.
[51] W. R. Entley, S. G. Girolami, *Science* **1995**, *268*, 397.
[52] S. Ferlay, T. Mallah, R. Ouahes, P. Veillet, M. Verdaguer, *Inorg. Chem.* **1999**, *38*, 229.
[53] W. D. Greibler, D. Babel, *Z. Naturforsch. B* **1982**, *87*, 832.
[54] D. Babel, *Comments Inorg. Chem.* **1986**, *5*, 285.
[55] R. Klenze, B. Kanellakopoulos, G. Trageser, H. H. Eysel, *J. Chem. Phys.* **1980**, *72*, 5819.
[56] W. E. Buschmann, J. S. Miller, *Inorg. Chem.* **2000**, *39*, 2411.
[57] L. G. Beauvais, J. R. Long, *J. Am. Chem. Soc.* **2002**, *124*, 12096.
[58] W. R. Entley, S. G. Girolami, *Inorg. Chem.* **1994**, *33*, 5165.
[59] K. Awaga, T. Sekine, M. Okawa, W. Fujita, S. M. Holmes, S. G. Girolami, *Chem. Phys. Lett.* **1998**, *293*, 352.
[60] S. Juszczyk, C. Johansson, M. Hanson, A. Ratuszna, G. Malecki, *J. Phys. Condens. Matter* **1994**, *6*, 5697.
[61] V. Gadet, M. Bujoli-Doeuff, L. Force, M. Verdaguer, K. El Malkhi, A. Deroy, J. P. Besse, C. Chappert, P. Veillet, J. P. Renard, P. Beauvillain, in *Magnetic Molecular Materials* (Eds.: D. Gatteschi, O. Kahn, J. S. Miller, F. Palacio), Kluwer Academic, Dordrecht, **1991**, p. 281.
[62] F. Herren, P. Fischer, A. Ludi, W. Hälg, *Inorg. Chem.* **1980**, *19*, 956.
[63] W. R. Entley, C. R. Treadway, G. S. Girolami, *Mol. Cryst. Liq. Cryst.* **1995**, *273*.
[64] V. Gadet, T. Mallah, I. Castro, M. Verdaguer, *J. Am. Chem. Soc.* **1992**, *114*, 9213.

Received: August 10, 2004
Published online: January 25, 2005